Inorganic Chemistry

Article

pubs.acs.org/IC

Mono- and Polynuclear Copper(II) Complexes of Alloferons 1 with Point Mutations (H6A) and (H12A): Stability Structure and Cytotoxicity

Mariola Kuczer,[†] Marta Błaszak,[†] Elzbieta Czarniewska,[‡] Grzegorz Rosiński,[‡] and Teresa Kowalik-Jankowska*[,†]

[†]Faculty of Chemistry, University of Wrocław, Joliot-Curie 14, 50-383 Wroclaw, Poland

[‡]Department of Animal Physiology and Development, Institute of Experimental Biology, Adam Mickiewicz University, Umultowska 89, 61-614 Poznan, Poland

Supporting Information

ABSTRACT: Mononuclear and polynuclear copper(II) complexes of the alloferons 1 (Allo1) with point mutations (H6A) $H^1GVSGA^6GQH^9GVH^{12}G$-COOH (Allo6A) and (H12A) $H^1GVSGH^6GQH^9GVA^{12}G$-COOH (Allo12A) have been studied by potentiometric, UV−visible, CD, EPR spectroscopic, and mass spectrometry (MS) methods. Complete complex speciation at different metal-to-ligand ratios ranging from 1:1 to 3:1 was obtained. At physiological pH 7.4 and a 1:1 metal-to-ligand molar ratio, the Allo6A and Allo12A peptides form CuL complexes with the 4N $\{NH_2, N_{Im}\text{-}H^1, 2N_{Im}\}$ binding mode. The amine nitrogen donor and the imidazole nitrogen atoms (H^9H^{12} or H^6H^9) can be considered to be independent metal-binding sites in the species formed for the systems studied. As a consequence, di- and trinuclear complexes for the metal-to-ligand 2:1 and 3:1 molar ratios dominate in solution, respectively. The induction of apoptosis *in vivo* in *Tenebrio molitor* cells by the ligands and their copper(II) complexes at pH 7.4 was studied. The biological results show that copper(II) ions *in vivo* did not cause any apparent apoptotic features. The most active was the Cu(II)−Allo12A complex formed at pH 7.4 with a $\{NH_2, N_{Im}\text{-}H^1, N_{Im}\text{-}H^6, N_{Im}\text{-}H^9\}$ binding site. It exhibited 123% higher of caspase activity in hemocytes than the native peptide, Allo1.

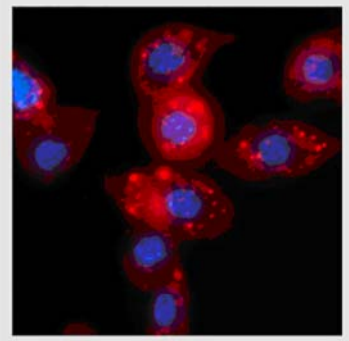

INTRODUCTION

Effective control of viral infections and diseases is limited, due to a relatively small number of efficient antiviral drugs.[1,2] It seems that natural compounds from plants, animals, and fungi present a promising strategy in the search for biological active compounds.[3−6] Until now, only eight peptides with antiviral activity have been isolated from insects.[7−13] One of them is alloferon, a novel insect tridecapeptide ($H\text{-}His^1\text{-}Gly\text{-}Val\text{-}Ser\text{-}Gly\text{-}His^6\text{-}Gly\text{-}Gln\text{-}His^9\text{-}Gly\text{-}Val\text{-}His^{12}\text{-}Gly\text{-}OH$) isolated in 2002 by Chernych from blow fly *Calliphora vicina*.[8] This short peptide contains four His residues in positions 1, 6, 9, and 12 and five Gly residues in positions 2, 5, 7, 10, and 13. Its primary structure is similar to that of some functionally relevant proteins, such as influenza virus B hemagglutinin, bovine prion protein I and II, and *Sarcophaga peregrina* antifungal protein. The *in vitro* experiments reveal that alloferon has a stimulatory activity toward natural killer lymphocytes.[8] *In vivo*, alloferon induces interferon (IFN) synthesis in mice.[8] A further study has shown that alloferon stimulates the synthesis of IFN through NF-*k*B activation.[14] Additional *in vivo* experiments in mice indicate that alloferon has both antiviral and antitumor capabilities.[8] Due to a unique immune modulating mechanism, alloferon may be used in conjunction with other antiviral and anticancer drugs to generate synergistic effects in combating disease. Structure/activity relationship studies of insect peptide alloferon by evaluating the antiviral effects of new alloferon analogues suggest that the presence of the aromatic ring in position 1 of the peptide chain can play a role in the expression of antiviral properties.[15,16]

Copper ions play a key role in a multitude of biological processes, mostly in the active center of enzymes where a major function is in electron transfer reactions and/or substrate binding. The imidazole moiety plays a particular role in the active center of a large number of (metallo)proteins. The stabilizing role of histidyl residues in the complex formation reactions of simple oligopeptides has already been well understood and thoroughly reviewed.[17−20] The coordination mode of His-containing peptides strongly depends on the number and position of the His residues in the peptide and those of the nearby donor groups.[17,20,21] For multihistidine peptides, all of the histidines can be considered to be independent metal-binding sites, and polynuclear complexes can be present even in equimolar samples of the metal ion and peptides, but the ratios of polynuclear species do not exceed the statistically expected ones.[22−27] Many essential metal ions act as the important factor influencing the structure of natural and synthetic oligopeptides, and as a consequence, they may have a

Received: January 21, 2013
Published: May 8, 2013

   dx.doi.org/10.1021/ic400160d | *Inorg. Chem.* 2013, 52, 5951−5961

critical impact on their biological activity.[28] Moreover, the copper–peptide complex may be more resistant to enzymatic degradation in comparison to that of free ligand.[29]

Recently, it was found that insect peptides such as *Neb*-colloostatin,[30] alloferon, and its selected analogues cause apoptosis in hemocytes of *T. molitor*.[31] Furthermore, several studies demonstrated that many Cu(II) complexes exhibit cytotoxic activity through cell apoptosis.[32] Also, heavy metals are known to be typical stimuli to trigger apoptosis in vertebrate and invertebrate cells.[33−35] It was demonstrated that Cu(II) strongly induces apoptosis *in vitro* in insect cells of *Aedes albopictus*.[34] This effect was maximal between 0.75 and 1 mM.

In this paper we report studies of the copper(II) complexes of (H6A) and (H12A) mutants of alloferon 1, H-His[1]-Gly-Val-Ser-Gly-His[6]-Gly-Gln-His[9]-Gly-Val-His[12]-Gly-OH (Allo1). These peptides contain three histidine residues ($H^1H^9H^{12}$) (Allo6A) and ($H^1H^6H^9$) (Allo12A). The copper(II) complexes were studied by the combined application of potentiometric equilibrium, spectroscopic (UV–visible, CD, EPR), and mass spectrometry methods in solution. Detailed description of the peptides' protonation constants and their Cu(II) complex speciations was obtained from a series of potentiometric measurements in the pH 2.5–10.5 range and at different metal-to-ligand molar ratios. ESI-MS (electrospray ionization mass spectrometry) aided the interpretation of the equilibria data by confirming the stoichiometry of the metal complexes formed. CD, UV–visible, and EPR spectroscopies were used to obtain complementary information concerning the number of coordinated nitrogen atoms as well as the geometry of the copper(II) complexes. The induction of apoptosis *in vivo* in insect cells of *Tenebrio molitor* by the ligands studied and their copper(II) complexes at pH 7.4 was also determined.

EXPERIMENTAL SECTION

Materials. Alloferons 1 with point mutations (H6A) and (H12A) were synthesized according to the procedure reported below. As a metal ion source $Cu(NO_3)_2{\cdot}3H_2O$ (Merck) was used. KNO_3, KOH, and HNO_3 were Merck products.

Synthesis of the Peptides. Peptides were synthesized by the classical solid phase method according to the Fmoc-procedure. Amino acids were assembled on a Fmoc-Gly-Wang resin. As a coupling reagent 2(1H-benzotriazole-1-yl)-1,1,3,3-tetramethyluronium hexafluorophosphate in the presence of 1-hydroxybenzotriazole was used. The N-Fmoc (Fmoc, 9-fluorenylmethoxycarbonyl) group was removed with 20% piperidine in *N*,*N*-dimethylformamide (DMF). The peptide-resin was cleaved with trifluoroacetic acid (TFA) in the presence of ethanedithiol. Both peptides were purified by preparative high performance liquid chromatography (HPLC) on a Varian ProStar, column-Tosoh Biosciences ODS-120T C18 (ODS 300 × 21.5 mm). Water–acetonitrile gradients containing 0.1% TFA at a flow rate of 7 cm^3/min were used for purification with UV detection at 220/240 nm. Analytical HPLC was performed with a Termo Separation Products with a VYDAC C_{18} column (ODS 250 mm × 4.6 mm) with a linear gradient of 0–100% B for 60 min at a flow rate of 1 mL/min determined at 220 nm. The molecular weights of the peptides were determined with a Bruker microTOF-Q mass spectrometer (Bruker, Daltonik, Germany).

Analytical data were as follows: alloferon with point mutations (H6A)(Allo6A) H^1GVSGA^{6}GQH^{9}GVH^{12}G-OH, R_t(HPLC) = 19.6 min, m/z $[M + H]^+$, found 1199.567 Da, calc 1199.5732 Da; $[M + 2H]^{2+}$ found 600.295 Da, calc 600.287 Da; $[M + 3H]^{3+}$ found 400.533 Da, calc 400.527 Da; (H12A)(Allo12A), H^1GVSGH^{6}GQH^{9}GVA^{12}G-OH, R_t(HPLC) = 19.8 min. m/z $[M + H]^+$ found 1199.5743 Da, calc 1199.5732 Da; $[M + 2H]^{2+}$ found 600.296 Da, calc 600.287 Da; $[M + 3H]^{3+}$ found 400.532 Da, calc 400.527 Da.

Potentiometric Measurements. Stability constants for proton and Cu(II) complexes were calculated from pH-metric titrations carried out in an argon atmosphere at 298 K using a total volume of 1.5–2 cm^3. Alkali was added from a 0.250 cm^3 micrometer syringe which was calibrated by both weight titration and the titration of standard materials. Experimental details: ligand concentration 1.25×10^{-3} M; metal-to-ligand molar ratio 1:1, 2:1, 3:1 for both ligands; ionic strength 0.10 M (KNO_3); $Cu(NO_3)_2$ was used as the source of the metal ions; pH-metric titration on a MOLSPIN pH-meter system using a Russell CMAW 711 semimicro combined electrode, calibrated in concentration using HNO_3,[36] number of titrations = 2; method of calculation: SUPERQUAD[37] and HYPERQUAD.[38] The samples were titrated in the pH region 2.5–10.5.

Protonation constants of the ligands and the overall stability constants ($\log \beta_{pqr}$) of the complexes were calculated by means of general computational programs[37,38] using eqs 1 and 2.

$$pM + qH + rL \leftrightarrow M_pH_qL_r \quad (1)$$

$$\beta_{pqr} = [M_pH_qL_r]/[M]^p[H]^q[L]^r \quad (2)$$

Titrations of the ligand in the presence of various equivalents of copper(II) were analyzed in batch calculations, in which all titration curves are fitted at the same time with one model. Standard deviations (values) quoted were computed by SUPERQUAD and HYPERQUAD and refer to random errors only. They are, however, a good indication of the importance of the particular species involved in the equilibria. The purities and exact concentration of the solutions of the ligand were determined by the method of Gran.[39]

Spectroscopic Studies. Solutions were of similar concentrations to those used in the potentiometric studies. Absorption spectra (UV–vis) were recorded on a Cary 50 "Varian" spectrophotometer in the 850–300 nm range. The spectra were scanned at the pH and stoichiometric M/L, values adequate to obtain the maximum formation of the particular species, but also in this condition, other species coexist in a smaller concentration. Electron paramagnetic resonance (EPR) spectra were performed in ethylene glycol–water (1:2, v/v) solution at 77 K on a Bruker ELEXSYS E500 CW-EPR spectrometer at the X-band frequency (~ 9.45 GHz) equipped with an ER 036TM NMR Teslameter and an E 41 FC frequency counter. The experimental spectra were simulated by using Bruker's WIN_EPR SimFonia Software Version 1.25. Circular dichroism (CD) spectra were recorded on a Jasco J-715 spectropolarimeter in the 750–250 nm range. The values of $\Delta\varepsilon$ (i.e., $\varepsilon_l - \varepsilon_r$) and ε (absorption spectra) were calculated at the maximum concentration of the particular species obtained from the potentiometric data.

ESI-MS Measurements. The mass spectra were obtained on a Bruker ESI-MS APEX_ULTRA spectrometer (Bruker Daltonik, Bremen, Germany) equipped with an Apollo II electrospray ionization source. The mass spectrometer was operated in the negative- or positive-ion mode. The instrumental parameters were as follows: scan range, m/z 250–2300; dry gas, nitrogen; temperature, 200 °C; reflector voltage, 1300 V; detector voltage, 1920 V. The samples were dissolved in water, and the 1:1, 2:1, and 3:1 metal-to-ligand molar ratios were prepared at pH about 7. pH was adjusted by addition of concentrated NaOH or HNO_3 solutions. The samples were infused at a flow rate of 3 μL/min. The instrument was calibrated externally with the Tunemix mixture (Bruker Daltonik, Germany) in quadratic regression mode.

Biological Investigation. *Insects.* A stock culture of *Tenebrio molitor* was maintained at the Department of Animal Physiology and Development as described previously.[40] Studies were carried out on 4-day old adult beetles. As the mealworm parents' age is important for the developmental features of their offspring,[41−43] all insects in our experiments derived from less than 1 month old parents.

The injection procedure, hemolymph collection, and *in situ* assay for activated caspases are described below.

The *T. molitor* beetles were anaesthetised with CO_2, washed in distilled water, and disinfected with 70% ethanol. The peptide, solution of copper(II) ions, and complex of copper(II) were prepared in MOPS

dx.doi.org/10.1021/ic400160d | Inorg. Chem. 2013, 52, 5951–5961

Table 1. Formation ($\log \beta$) and Protonation ($\log K$) Constants for Allo6A and Allo12A, and Comparable Peptides at T = 298 K

	I = 0.1 (KNO_3)			I = 0.1 M (NaCl)
	Allo6A	Allo12A	Alloferon 1[a]	HADHDHKK[b]
		$\log \beta$		
HL	7.67 ± 0.02	7.49 ± 0.01	7.64 ± 0.01	10.80
H_2L	14.53 ± 0.02	14.15 ± 0.01	14.58 ± 0.01	20.96
H_3L	20.76 ± 0.02	20.13 ± 0.01	21.04 ± 0.01	28.51
H_4L	26.01 ± 0.02	25.31 ± 0.01	26.95 ± 0.01	35.16
H_5L	29.07 ± 0.02	28.85 ± 0.01	32.11 ± 0.01	41.18
H_6L			35.30 ± 0.01	46.37
H_7L				49.96
H_8L				52.70
		$\log K$		
NH_2-Lys				10.80
NH_2-Lys				10.16
NH_2- terminal	7.67	7.49	7.64	7.55
N_{im}	6.86	6.66	6.94	6.65
N_{im}	6.23	5.98	6.46	6.02
N_{im}	5.25	5.18	5.91	5.19
N_{im}			5.16	
COO^-	3.06	3.54	3.19	3.59
COO^-				2.70

[a]Reference 54. [b]Reference 50.

buffer at pH 7.4 (Sigma-Aldrich, MOPS 3-(*N*-morpholino)-propanesulfonic acid),[44] and these solutions were injected (2 μL, in dose of 10 nM of peptide per insect) through the ventral membrane between the second and the third abdominal segments toward the head with a Hamilton syringe (Hamilton Co.). The control insects were injected with the same volume of physiological saline (control 1), MOPS (control 2), or MOPS + Cu (control 3). All solutions were sterilized through the 0.22 μm pore filter membrane (Millipore), and all injections were performed under sterile conditions.

Before hemolymph collection, the beetles were anaesthetized again with CO_2, washed in distilled water, and disinfected with 70% ethanol. Both control and injected insects were taken 1 h after injection, and the hemocytes were prepared. Upon cutting off a tarsus from a foreleg, hemolymph samples (5 μL) were collected with "end to end" microcapillaries (Drummond). They were diluted in 20 μL of ice-cold physiological saline containing anticoagulant buffer (4.5 mM citric acid and 9 mM sodium citrate) in a 5:1 v/v ratio. Hemolymph from control- and from peptide-injected insects was dropped on alcohol-cleaned cover glasses coated with 7 μL of 0.01% poly-L-lysine (Sigma P4707). After allowing hemocytes to settle (15 min, at room temperature), the remaining fluid was removed, and the remaining cells were washed twice with physiological saline. The prepared hemocytes were used for the microscopic analysis of activation of caspases.

The presence of active caspases was searched for by using a sulphorhodamine derivative of valylalanylaspartic acid fluoromethyl ketone, a potent inhibitor of caspase activity (SR-VAD-FMK) (in accordance with the manufacturer's instructions of the sulphorhodamine multicaspase activity kit, AK-115, BIOMOL, PA). In this kit, sulforhodamine labeled valylalanylaspartic acid fluoromethyl ketone (SR-VAD-FMK) enters the cell and acts as a specific inhibitor of apoptosis by covalently binding to the reactive cysteine residue indicative of anactive caspase. The sulforhodamine label allows detection and localization of active caspases by fluorescence microscopy. Hemocytes were incubated in reaction with 1:3 v/v SR-VAD-FMK to physiological saline for 1 h at room temperature in the dark, rinsed again three times with wash buffer for 5 min at room temperature, and finally fixed in 3.7% paraformaldehyde for 10 min. After washing again in physiological saline, the hemocytes were stained with DAPI (4′,6-diamidino-2-phenylindole). Incubation in the dark lasted for 5 min. Thereafter, the hemocytes were washed once with distilled water, and they were mounted using a mounting medium. The prepared hemocytes were studied with a Nikon Eclipse TE 2000-U fluorescence microscope with filters set for rhodamine (excitation 543 nm and emission 560 nm), and the intensity of fluorescence of the apoptosing cells was measured by using an NIS-Element AR 3.1 program. The changes in fluorescence intensity were used to quantify caspase activities. Data were shown as mean ± SD. A percentage of apoptotic hemocytes [(number of apoptotic cells − fluorescent cells)/number all cells × 100%] was calculated from at least 50 cells (all) in each experiment. These data were obtained from three independent experiments. The same method of studying the pro-apoptic effects of peptide hormones in insects was used in our previous papers.[30,31,45]

RESULTS AND DISCUSSION

Protonation Equilibria of the Ligands. Protonation ($\log K$) and formation ($\log \beta$) constants of the ligands Allo6A and Allo12A are collected in Table 1, and the parameters of Alloferon 1 and HADHDHKK peptides are also shown for comparison. It is clear from Table 1 that the peptides studied have five protonation sites which can be assigned to the N-terminal amino, three imidazole nitrogen atoms, and C-terminal carboxylate functions. In agreement with the common oligopeptides, the terminal amino groups are the most basic sites of these ligands, while the C-terminal α-carboxylic groups are the most acidic. The protonation constants of the N-terminal group ($\log K$ 7.49; 7.67, Table 1) are comparable to those of the peptides containing the N-terminal His residue (HSDGI-NH_2,[46] HGG,[47] Neurokinin A[48]). For both peptides, three $\log K$ values (6.86−5.18, Table 1) are in the range of basicity of the imidazole ring.[49,50] For both peptides, the difference of the three $\log K$ values is rather small (0.63−0.98), suggesting that protonation of the histidine residues takes place in overlapping processes. Therefore, these constants are very likely macroconstants containing contributions from protonation of three histidines and cannot be assigned to a specific histidyl residue.[23,51] The other protonation constants are of the C-terminal carboxyl groups with the stepwise values ($\log K$) 3.06 and 3.54 for Allo6A and Allo12A, respectively (Table 1).[52] Although the sequences of studied peptides are similar (the difference is only in the substitution His → Ala in one position

dx.doi.org/10.1021/ic400160d | Inorg. Chem. 2013, 52, 5951−5961

Table 2. Stability Constants (log β) of Mononuclear Copper(II) Complexes of Allo6A and Allo12A, and Comparable Peptides at T = 298 K, and Calculated Deprotonation Constants for Histidine and Amide Protons (pK) in Cu(II) Complexes

	I = 0.1 (KNO_3)			I = 0.1 M (NaCl)
species	Allo6A	Allo12A	Alloferon 1[a]	HADHDHKK[b]
$[CuH_5L]$				46.29
$[CuH_4L]$				42.30
$[CuH_3L]$	25.66 ± 0.11		28.10 ± 0.02	38.71
$[CuH_2L]$	22.17 ± 0.04	20.95 ± 0.03	23.96 ± 0.01	33.66
$[CuH_1L]$	17.80 ± 0.05	16.40 ± 0.02	18.95 ± 0.01	
[CuL]	12.33 ± 0.05	10.90 ± 0.03	12.60 ± 0.02	17.17
$[CuH_{-1}L]$	3.74 ± 0.06	2.72 ± 0.04	3.67 ± 0.03	7.16
$[CuH_{-2}L]$			−5.13 ± 0.02	−3.63
$[CuH_{-3}L]$	−14.82 ± 0.08	−15.07 ± 0.04	−14.27 ± 0.02	−15.60
$[CuH_{-4}L]$	−24.92 ± 0.06	−24.90 ± 0.03	−25.13 ± 0.04	
pK (His)	3.49		4.14	3.99
pK(His)	4.37	4.55	5.01	3.59
pK(His)	5.47	5.50		5.05
pK_1 (amide)	8.59	8.18	8.93	8.25
pK_2 (amide)	9.28	8.90	8.80	8.25
pK_3 (amide)	9.28	8.90	9.14	10.10

[a]Reference 54. [b]Reference 50.

Table 3. Stability Constants (log β) of Polynuclear Copper(II) Complexes of Allo6A and Allo12A at T = 298 K and I = 0.1 (KNO_3) and Calculated Deprotonation Constants for Amide Protons (pK) in Cu(II) Complexes

species	Allo6A	Allo12A	species	Allo6A	Allo12A
$[Cu_2H_{-1}L]$			$[Cu_3H_{-4}L]$	−7.78 ± 0.12	−7.26 ± 0.06
$[Cu_2H_{-2}L]$	2.70 ± 0.06	2.67 ± 0.03	$[Cu_3H_{-5}L]$	−14.63 ± 0.07	−14.06 ± 0.04
$[Cu_2H_{-3}L]$	−4.21 ± 0.06	−4.51 ± 0.04	$[Cu_3H_{-6}L]$	−22.49 ± 0.07	−21.90 ± 0.05
$[Cu_2H_{-4}L]$	−12.38 ± 0.06	−12.48 ± 0.04	$[Cu_3H_{-7}L]$		−30.52 ± 0.05
$[Cu_2H_{-5}L]$	−21.44 ± 0.07	−21.85 ± 0.05	$[Cu_3H_{-8}L]$	−39.83 ± 0.07	−40.15 ± 0.07
$[Cu_2H_{-6}L]$	−30.94 ± 0.07	−31.99 ± 0.09	$[Cu_3H_{-9}L]$		−49.88 ± 0.06
$[Cu_2H_{-7}L]$	−40.81 ± 0.07	−42.51 ± 0.09	$[Cu_3H_{-10}L]$	−58.71 ± 0.07	
pK_3 (amide)	6.91	7.18	pK_5 (amide)	6.86	6.80
pK_4 (amide)	8.17	7.97	pK_6 (amide)	7.85	7.84
pK_5 (amide)	9.06	9.37	pK_7 (amide)	8.67	8.62
pK_6 (amide)	9.50	10.14	pK_8 (amide)	8.67	9.63
			pK_9 (amide)	9.44	9.73

Table 4. Calculated log K^* [a] Values for Mononuclear Copper(II) Complexes with Allo6A and Allo12A and Comparable Ligands

log K^* [a]	1N	2N {NH_2,N_{Im}-His[1]}	3N {NH_2,N_{Im}-His[1]+N_{Im}}	4N {NH_2, 3N_{Im}}	4N {N_{Im},3N^-}	4N {NH_2,3N^-}
Allo6A	−0.35	−3.84	−8.21	−13.68	−20.07	−22.49
Allo12A		−4.36	−8.91	−14.41	−20.25	−22.56
Alloferon 1[b]		−4.01	−8.15	−13.16	−19.43	−21.91
HADHDHKK[c]	−0.08	−4.07	−7.66	−12.71	−18.99	−21.35

[a]log K^* = log β (CuH_jL) − log β (H_nL) (where the index j corresponds to the number of protons in the ligand coordinated to the metal ion and n corresponds to the number of protons coordinated to the ligand). [b]Reference 54. [c]Reference 50.

of the peptides), the protonation constants of the carboxylate groups are different by about 0.5 log units (Table 2). This difference may result from different conformations of the peptides and the formation of the hydrogen bonds.

Copper(II) Complexes. The stability of the complexes formed in the Cu(II)−Allo6A and Cu(II)−Allo12A systems was determined by analysis of the potentiometric studies carried out at different metal-to-ligand molar ratios (1:1, 2:1, and 3:1). Different species were considered, but the best model with the stoichiometries (charges have been omitted for clarity) reported in Tables 2 and 3 was chosen. The results clearly show that the peptides studied can keep 3 equiv of metal ions in solution according to the number of anchoring sites in the molecules [amine or histidine residues in the first position and two imidazole nitrogens of His (H^9,H^{12} or H^6,H^9) residues]. The precipitation was not observed at any pH value and at metal-to-ligand molar ratios from 1:1 to 3:1. This is an indirect proof for the formation of mono-, di-, and trinuclear species in solution, and both computer calculation of potentiometric data and spectroscopic measurements support this assumption. The log K^* values for mononuclear complexes corresponding to the protonation corrected stability constants, which are useful in comparing the ability of various ligands to bind a metal ion, are given in Table 4.[53] Figures 1−3 and S1−S3 demonstrate that the mononuclear complexes are mainly present in equimolar

dx.doi.org/10.1021/ic400160d | Inorg. Chem. 2013, 52, 5951−5961

samples, while polynuclear species predominate at the 2:1 and 3:1 ratios.

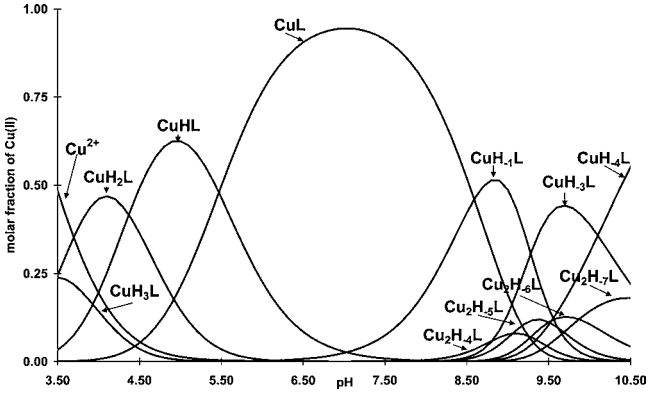

Figure 1. Concentration distribution of the complexes formed in the copper(II)−Allo6A system as a function of pH. Cu(II)-to-peptide molar ratio 1:1, [Cu(II)] = 0.001 M.

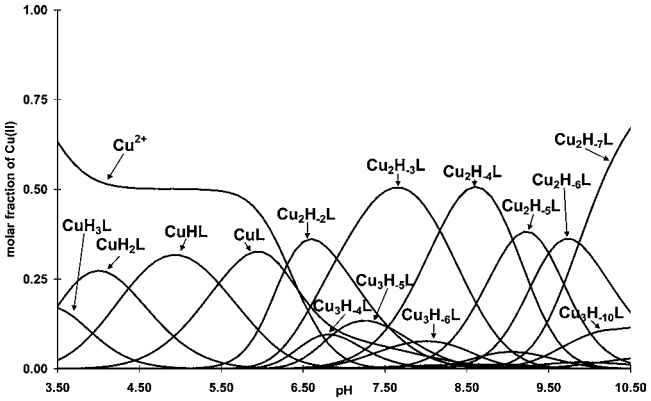

Figure 2. Concentration distribution of the complexes formed in the copper(II)−Allo6A system as a function of pH. Cu(II)-to-peptide molar ratio 2:1, [Cu(II)] = 0.002 M.

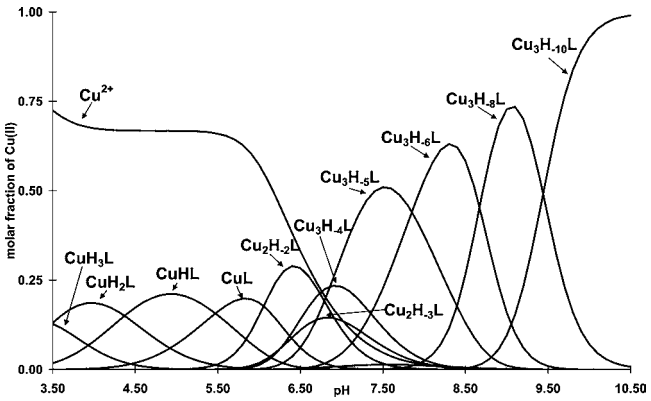

Figure 3. Concentration distribution of the complexes formed in the copper(II)−Allo6A system as a function of pH. Cu(II)-to-peptide molar ratio 3:1, [Cu(II)] = 0.003 M.

From potentiometric data calculations, seven and six monocomplexes are found for the Cu(II)−Allo6A and Cu(II)−Allo12A systems, respectively (Table 2; Figures 1 and S1 (figures with "S" preceding the figure number are in the Supporting Information). In the solutions containing a 1:1 metal-to-ligand molar ratio, the following species are present: CuH_3L (only for Cu(II)−Allo6A), CuH_2L, CuHL, CuL, $CuH_{-1}L$, $CuH_{-3}L$, and $CuH_{-4}L$ (Table 2, Figures 1 and S1; charges omitted for simplicity). The CuH_3L species of the Allo6A is present in low concentration and cannot be characterized by spectroscopic methods. However, for the CuH_3L complex, the stoichiometry and log K^* value (Table 4) correspond to the formation of the 1N {NH_2 or N_{Im}} binding site. With increasing pH, the CuH_2L species is formed for both peptides. In UV−visible spectra, the d−d transition energy at 669−671 nm (Figure S4; Tables 5 and 6), in CD spectra of the $N_{Im}(\pi_2) \rightarrow$ Cu(II) charge transfer transition at 280 nm (Table 6), is consistent with the histamine coordination mode 2N {NH_2,N_{Im}-His[1]} of the Allo6A and Allo12A to copper(II) ions.[46,54−56] Coordination of histidine normally gives charge transfer transitions at ∼260 and ∼330 nm.[57] The band at about 280 nm is also attributed to the $NH_2 \rightarrow$ Cu(II) LMCT.[58,59] Therefore, in CD spectra the band at ∼260−280 nm may be assigned to the $NH_2 \rightarrow$ Cu(II) and $N_{Im}(\pi_2) \rightarrow$ Cu(II) charge transfer LMCT transitions (Tables 5 and 6). The magnitude and precise energy of the charge transfer transitions for an imidazole nitrogen to Cu(II) are very sensitive to the position of the ring plane relative to the complex plane and, thus, to the possibility of its rotation.[57] With increasing pH, the deprotonation and coordination of the subsequent imidazole nitrogen atoms of histidine residues occur. At pH 5, the CuHL complexes dominate, with the following spectroscopic parameters: the d−d energy at 627−630 nm and the EPR parameters A_{II} 160−171 G and g_{II} 2.266−2.272 (Figure S5; Tables 5 and 6), which correspond to three nitrogen donor atoms coordinated to copper(II) ions.[50,54] The deprotonation and coordination of the imidazole nitrogen atoms occur with pK values 5.47−5.50 (Table 2), and the CuL species are present in the wide pH range 5.5−8.5. The shift of the absorption maximum to 605−606 nm (Figure S4) and the EPR parameters A_{II} 184 G and g_{II} 2.246 (Figure S5) suggest coordination mode 4N {NH_2,N_{Im}-His[1],2N_{Im}} to copper(II) ions (Tables 5 and 6).[22,60,61] The log K^* value for the CuL complex of the Allo6A is higher by about 0.7 log unit in comparison to that of the Allo12A but is comparable to that of the Alloferon 1 (Table 4). The stabilization of the 4N complex of Allo6A compared to that of Allo12A may result from the size of the macrochelate as well as from the structural organization (by the formation of the hydrogen bonds) of the peptide in copper(II) complexes.[62] Lack of the d−d transitions in CD spectra for the complexes formed in the 3.5−8.5 pH range may support coordination of the imidazole nitrogen of the histidine residues rather than amide nitrogens (Tables 5 and 6).[63,64] This is indirect proof for coordination of the metal ion by the side chain histidine residues, which are rather far from the chirality centers of the molecules. The second proof for the coordination mode 4N {NH_2,N_{Im}-His[1],2N_{Im}} (Scheme 1a) to copper(II) ion is a high value first deprotonation of amide nitrogen atoms (8.18−8.59, Table 2), while for the HSDGI-NH_2 peptide this value is equal to 6.35.[46] It should be mentioned that at physiological pH (7.4) the CuL complex with 4N {NH_2,N_{Im}-His[1],2N_{Im}} binding sites dominates. With increasing pH above 8.50, the sequential deprotonation and coordination of amide nitrogen donors occur, with the formation of the 4N {NH_2,3N^-} or {N_{Im},3N^-} complexes. In UV−visible spectra, the shift of the absorption maximum to 525−547 nm (Figure S4), and the EPR parameters A_{II} 198−212 G and g_{II} 2.190−2.202 (Figure S5) suggest the coordination of the additional nitrogen donor atoms with the formation of the 4N complexes with amide

dx.doi.org/10.1021/ic400160d | Inorg. Chem. 2013, 52, 5951−5961

Table 5. Spectroscopic Data for the Mononuclear and Polynuclear Cu(II) Complexes of Allo6A

			UV−vis		CD		EPR	
system	species	pH	λ (nm)	ε (M^{-1} cm^{-1})	λ (nm)	$\Delta\varepsilon$ (M^{-1} cm^{-1})	A_{II} (G)	g_{II}
1:1	CuH_2L 2N $\{NH_2,N_{Im}\text{-}His^1\}$	4.0	669[a]	29				
	$CuHL$ 3N $\{NH_2,N_{Im}\text{-}His^1 + N_{Im}\}$	5.0	627[a]	46			171	2.266
	CuL 4N $\{NH_2,N_{Im}\text{-}His^1 + 2N_{Im}\ (His^9,His^{12})\}$	7.0	605[a]	61			184	2.246
	$CuH_{-3}L$ 4N $\{NH_2,3N^-\}$ or $\{N_{Im},3N^-\}$	9.9	525[a]	102	589[a]	−0.412	198	2.202
					495[a]	0.835		
					310[b]	−0.864		
					279[c,d]	0.167		
2:1	$Cu_2H_{-3}L$ 2N,4N $\{NH_2,N^-,CO\}$ $\{N_{Im},2N^-,N_{Im}\}$ or 3N,3N $\{NH_2,2N^-,CO\}$ $\{N_{Im},N^-,N_{Im}\}$	7.3	605[a]	65	598[a]	−0.036	182	2.250
					510[a]	0.271		
					352[e]	0.102		
					305[b]	−0.260		
	$Cu_2H_{-7}L$ 4N,4N $\{NH_2,3N^-\}$ $\{N_{Im},3N^-\}$	10.5	522[a]	115	585[a]	0.411	198	2.188
					494[a]	0.694		
					310[b]	−0.790		
3:1	$Cu_3H_{-5}L$ 2N,3N,3N $\{NH_2,N^-,CO\}$ $\{N_{Im},2N^-\}$ $\{N_{Im},2N^-\}$ or 3N,3N,2N $\{NH_2,2N^-,CO\}$ $\{N_{Im},2N^-\}$ $\{N_{Im},N^-\}$	7.5	589[a]	72	602[a]	−0.118	broad band Cu(II)−Cu(II) interaction	
					509[a]	0.294		
					351[e]	0.098		
					306[b]	−0.374		
	$Cu_3H_{-6}L$ 3N,3N,3N $\{NH_2,2N^-,CO\}$ $\{N_{Im},2N^-\}$ $\{N_{Im},2N^-\}$	8.3	580[a]	86	595[a]	−0.202	broad band, Cu(II)−Cu(II) interaction with spectrum	
					505[a]	0.378		
					354[e]	0.092		
					306[b]	−0.494		
							184	2.240
	$Cu_3H_{-8}L$ 3N,4N,4N $\{NH_2,2N^-,CO\}$ $\{N_{Im},3N^-\}$ $\{N_{Im},3N^-\}$	9.2	569[a]	82	592[a]	−0.261	broad band Cu(II)−Cu(II) interaction	
					500[a]	0.430		
					357[e]	0.078		
					309[b]	−0.527		
	$Cu_3H_{-10}L$ 4N,4N,4N $\{NH_2, 3N^-\}$ $\{N_{Im},3N^-\}$ $\{N_{Im},3N^-\}$	10.5	531[a]	101	589[a]	−0.329	broad band, Cu(II)−Cu(II) interaction with spectrum	
					496[a]	0.523		
					360[e]	0.059		
					309[b]	−0.649		
							205	2.189

[a] d−d transition. [b] N_{amide} → Cu(II) charge transfer transition. [c] NH_2 → Cu(II) charge transfer transition. [d] N_{Im} (π_2) → Cu(II) charge transfer transition. [e] N_{Im} (π_1) → Cu(II) charge transfer transition.

nitrogens coordinated to copper(II) ions (Tables 5 and 6). The absorption maximum for the $CuH_{-3}L$ complex of Allo12A at 547 nm, ε_{max} 161 M^{-1} cm^{-1}, which is significantly red-shifted as compared to that of the Allo6A, can be explained by the axial interaction of the side chain imidazole nitrogen atoms.[19] The parameters of UV−visible, CD, and EPR spectra are not altered in basic solution (9.5−10.5 pH range), suggesting the same coordination binding in the $CuH_{-3}L$ and $CuH_{-4}L$ complexes (Figures 1 and S1). Therefore, the formation of the $CuH_{-4}L$ species can be assigned to the further deprotonation of the N^1-pyrrolic nitrogen in the imidazole ring without metal coordination.[65] As is seen in Figures 1 and S1 for pH above 8.5, in equimolar Cu(II)−Allo6A and Cu(II)−Allo12A systems, the dimeric complexes are also formed.

The ESI-MS spectra obtained for the Cu(II)−Allo6A and Cu(II)−Allo12A 1:1 metal-to-ligand molar ratio systems recorded in the positive mode show dominant signals for the $[CuL]^{2+}$ (630.7 Da, m/z), $[Cu_2H_{-2}L]^{2+}$ (661.2 Da, m/z), $[Cu_3H_{-4}L]^{2+}$ (692.7 Da, m/z), and even $[Cu_4H_{-6}L]^{2+}$ (723.1 Da, m/z) (Figure 4), supporting the formation of the mono- and polynuclear complexes in the MS experimental conditions. It should be mentioned that the conditions of the formation of the complexes in solution and the conditions in the MS experiment are quite different. In solution with a 1:1 metal-to-ligand molar ratio, the mononuclear complexes dominate while in the MS experiment the polynuclear complexes (even in very small concentrations) may be observed. The ESI-MS mass spectrum for the Cu(II)−Allo6A 1:1 molar ratio system shows a dominant signal for the $[CuHL]^{3+}$ molecular ion with the m/z value 420.8 Da (Figure 6S). The ESI-MS method has been used in a wide variety of fields to study the formation, stoichiometry, and speciation of metal complexes of organic ligands.[66,67]

The anchoring and binding sites of peptides studied are well separated, and the polynuclear complexes can be formed. Then, the copper(II) ions may be coordinated independently from each other by donor atoms of the peptide backbone.[68,69]

Figures 2 and S2 present the metal ion speciation in the samples at a 2:1 copper(II)-to-ligand molar ratio. As is seen in Figures 2 and S2, the mononuclear complexes dominate at low (3.5−6) pH range, while they are dinuclear at higher (6−10.5) pH range. Trinuclear species are also formed but with molar fraction of Cu(II) not more than 10% (Figures 2 and S2). For the Cu(II)−Allo6A 2:1 molar ratio, the $Cu_2H_{-3}L$ and $Cu_2H_{-7}L$ complexes dominate in solution. At pH 7.5, the $Cu_2H_{-3}L$

dx.doi.org/10.1021/ic400160d | Inorg. Chem. 2013, 52, 5951−5961

Table 6. Spectroscopic Data for the Mononuclear and Polynuclear Cu(II) Complexes of Allo12A

			UV−vis		CD		EPR	
system	species	pH	λ (nm)	ε (M^{-1} cm^{-1})	λ (nm)	$\Delta\varepsilon$ (M^{-1} cm^{-1})	A_{II} (G)	g_{II}
1:1	CuH_2L 2N $\{NH_2,N_{Im}\text{-}His^1\}$	4.0	671[a]	52	280[c,d]	0.063		
	$CuHL$ 3N $\{NH_2,N_{Im}\text{-}His^1,N_{Im}\}$	5.0	630[a]	128			160	2.272
	CuL 4N $\{NH_2,N_{Im}\text{-}His^1 + 2N_{Im}\}$	7.0	606[a]	144			176	2.254
	$CuH_{-4}L$ 4N $\{NH_2,3N^-\}$ or $\{N_{Im},3N^-\}$	10.5	547[a]	161	606[a]	−0.183	212	2.190
					505[a]	+0.513		
					277[c,d]	broad band		
2:1	$Cu_2H_{-2}L$ $\{NH_2,N_{Im}\text{-}His^1\}$ $\{N_{Im},2N^-,N_{Im}\}$ or $NH_2,N_{Im}\text{-}His^1,N_{Im}\}$ $\{N_{Im},2N^-\}$	6.4	605[a]	81			176	2.254
	$Cu_2H_{-4}L$ $\{NH_2,2N^-,CO\}$ $\{N_{Im},2N^-,N_{Im}\}$	8.6	589[a]	104	781[a]	0.159	broad band Cu(II)−Cu(II) interaction	
					597[a]	−0.151		
					508[a]	0.213		
					352[e]	0.690		
	$Cu_2H_{-6}L$ $\{NH_2,3N^-\}$ $\{N_{Im},2N^-\}$	10.3	533[a]	128	779[a]	0.169	205	2.200
					599[a]	−0.131		
					503[a]	0.313		
					288[c,d]	−0.083		
3:1	$Cu_3H_{-5}L$ 2N,3N,3N $\{NH_2,2N^-,CO\}$ $\{N_{Im},N^-\}$ $\{N_{Im},2N^-\}$	7.4	598[a]	89	779[a]	0.156	174	2.255
					606[a]	−0.041		
					521[a]	0.100		
					350[e]	0.082		
	$Cu_3H_{-9}L$ 4N,4N,4N $\{NH_2,3N^-\}2\times\{N_{Im},3N^-\}$	10.5	532[a]	117	781[a]	0.141	broad band Cu(II)−Cu(II) interaction	
					602[a]	−0.097		
					509[a]	0.226		
					293[b]	−0.132		

[a]d−d transition. [b]N_{amide} → Cu(II) charge transfer transition. [c]NH_2 → Cu(II) charge transfer transition. [d]N_{Im} (π_2) → Cu(II) charge transfer transition. [e]N_{Im} (π_1) → Cu(II) charge transfer transition.

Scheme 1. [CuL] Complex with 4N $\{NH_2,N_{Im}\text{-}H^1,N_{Im}\text{-}H^9,N_{Im}\text{-}H^{12}\}$ Coordination of Allo6A (a) and $[Cu_3H_{-9}L]$ Complexes with $\{NH_2,3N^-\}$, $2\times\{N_{Im},3N^-\}$ Coordination of Allo6A and Allo12A (b)

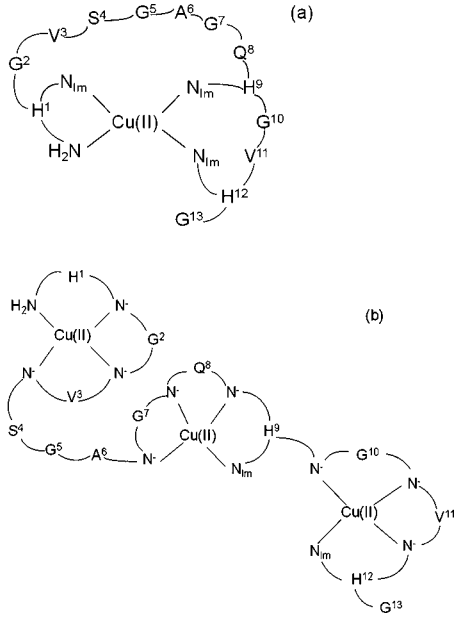

complex exists in ∼50%. The EPR parameters A_{II} 182 G and g_{II} 2.250, the absorption band of the d−d transition at 605 nm, and the presence in the CD spectrum of N_{Im} → Cu(II) and $N(amide)^-$ → Cu(II) charge transfer transitions at 352 and 305 nm (Table 5), respectively, suggest the 3N coordination modes

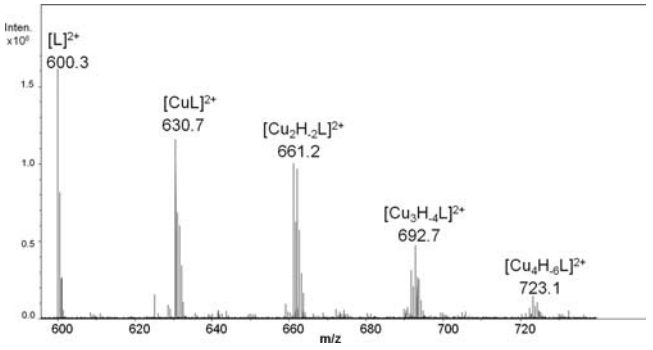

Figure 4. ESI mass spectrum for the Cu(II)−Allo12A system at 1:1 molar ratio in water solution at pH about 7.

of copper(II) ions with the imidazole nitrogen atom of the histidine residues and amide nitrogen atoms. At pH above 9, the $Cu_2H_{-7}L$ complex is formed (Figure 2). Formation of this species is accompanied by a significant blue shift of the absorption band to 522 nm (Table 5), suggesting coordination of the additional nitrogen donors. The EPR A_{II} 198 G, g_{II} 2.188, and UV−visible parameters (d−d transition at 522 nm, Table 5) suggest the presence in the $Cu_2H_{-7}L$ complex of the 4N $\{NH_2,3N^-\}$ and 4N $\{N_{Im},3N^-\}$ coordination modes around two copper(II) ions. The deprotonation of the $Cu_2H_{-6}L$ species to the $Cu_2H_{-7}L$ complex with pK value 9.87 (Table 3) may correspond to the deprotonation of the N^1-pyrrolic nitrogen in the imidazole ring without metal coordination.[65]

For the 2:1 metal-to-ligand molar ratio of the Cu(II)−Allo12A system, the $Cu_2H_{-2}L$ and $Cu_2H_{-4}L$ complexes dominate (Figure S2) in the 5.5−7 and 8−9 pH ranges,

dx.doi.org/10.1021/ic400160d | Inorg. Chem. 2013, 52, 5951−5961

respectively. The stoichiometry of the $Cu_2H_{-2}L$ complex and the spectroscopic parameters of UV−visible, CD, and EPR spectra may suggest the 2N $\{NH_2,N_{Im}\text{-}H^1\}$ 4N $\{N_{Im},2N^-,N_{Im}\}$ or 3N $\{NH_2,N_{Im}\text{-}H^1,N_{Im}\}$ 3N $\{N_{Im},N^-,N_{Im}\}$ binding modes around two metal ions (Table 6). With increasing pH, the $Cu_2H_{-2}L$ complex lost two protons and the $Cu_2H_{-4}L$ species is formed. The d−d transition is blue-shifted, suggesting the coordination of the sequential amide nitrogens with the formation of 3N $\{NH_2,2N^-,CO\}$ 4N $\{N_{Im},2N^-,N_{Im}\}$ binding sites for two metal ions. As is seen in Table 3, the p*K*(amide) values for the Cu(II)−Allo6A and Cu(II)−Allo12A 2:1 systems are similar to each other. The log *K** values of the Cu(II)−Allo6A (−43.86) and Cu(II)−Allo12A (−44.66) systems suggest higher stability of the $Cu_2H_{-6}L$ complex of the Allo6A peptide in comparison to that of the Allo12A. Because the Allo6A and Allo12A peptides contain two imidazole nitrogen atoms besides the His^1 residue (His^9, His^{12} or His^6, His^9), and in the $Cu_2H_{-7}L$ and $Cu_2H_{-6}L$ complexes, respectively, only one of them is coordinated, the coordination isomers cannot be excluded.[70] The presence of the coordination isomers and the difference in the ratio of these isomers are seen in the difference of the speciation of these two 2:1 systems.

The ESI-MS spectra for the Cu(II)−Allo12A system at a 1:1 molar ratio in water solution at pH about 7 recorded in positive mode show a signal for the dinuclear $[Cu_2H_{-2}L]^{2+}$ molecular ion (*m*/*z* 662.2 Da), supporting formation of polynuclear complexes in the MS experimental conditions (Figure S7).

For the 3:1 metal-to-ligand molar ratio, mono-, di-, and trinuclear complexes are formed for both peptides (Figures 3 and S3). The mononuclear complexes form at pH 3.5−6, dinuclear at 5.5−7, and trinuclear at pH higher than 6.5. As is seen on the distribution diagrams (Figures 3 and S3) because of the overlapping of the species formed, the complexes cannot be characterized accurately. Therefore, in Tables 5 and 6, the spectroscopic parameters are given at pH where the species dominate and the coordination modes are proposed. With increasing pH the absorption band of the d−d transitions is blue-shifted indicating the coordination of the subsequent amide nitrogen donors to copper(II) ions. At pH above 9.5 the $Cu_3H_{-9}L$ and $Cu_3H_{-10}L$ complexes are dominanted for the Cu(II)-Allo12A and Cu(II)-Allo6A systems, respectively (Figures 3 and S3). In UV−visible spectra the transition energy of the d−d transition at 531−532 nm and the stoichiometry of the complexes suggest the 4N $\{NH_2,3N^-\}$ 2×4N $\{N_{Im},3N^-\}$ coordination modes for three copper(II) ions (Scheme 1). For the trinuclear complexes, significant EPR line broadening is observed, although for the $Cu_3H_{-5}L$, $Cu_3H_{-9}L$ complexes of the Allo6A and the $Cu_3H_{-5}L$ species of Allo12A the EPR parameters could be determined. Significant EPR line broadening (Figure S8) suggests some spin−spin interactions between the coordinated Cu(II) ions, indicating that paramagnetic Cu(II) ions are close to each other. The broadening of the EPR line may be due to dipolar as well as exchange interaction between Cu(II) ions.[71] The exchange interaction produces the collapse of the four hyperfine lines, according to the Anderson exchange model.[72] Because the observed line width does not change by increasing or decreasing the concentration (data not shown), this indicates an association of the complexes into larger aggregates, leading to the concentration-independent line broadening by dipolar interactions.[73]

The obtained ESI-MS spectra for the Cu(II)−Allo12A system at a 1:1 molar ratio in water solution at pH 7 recorded in positive mode show a dominant signal for the $[Cu_3H_{-4}L]^{2+}$ molecular ion (*m*/*z* 692.7 Da), supporting formation of the trinuclear complexes under the MS experimental conditions (Figure 5). It should also be mentioned that for the Cu(II)−

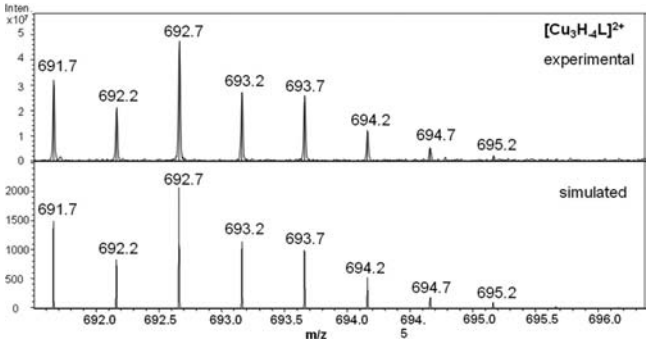

Figure 5. ESI mass spectrum for the Cu(II)−Allo12A system at 1:1 molar ratio in water solution at pH about 7. Experimental and simulated spectra for the $[Cu_3H_{-4}L]^{2+}$ molecular ion with *m*/*z* 692.7 Da.

Allo12A 1:1 system at pH 7 the signal of the $[Cu_4H_{-6}L]^{2+}$ species (*m*/*z* 723.1 Da) was also observed (Figure S9). This suggests that for the systems studied in MS experimental conditions the polynuclear complexes (even tetranuclear; anchoring sites of the peptides: amine and three imidazole nitrogen atoms) are easily formed and ionized.

It should be mentioned that the apparent binding constant of the first site was estimated and it is in the low micromolar range (6×10^{-6} M). The affinity of the second and third site cannot be calculated from the data of potentiometric measurements and their calculations. However, it may be stated that the second and third binding sites will be weaker in comparison to that of the first, and likely never occupied under physiological conditions, because there is not enough Cu(II) available.

Biological Activity. In *in vivo* bioassay using the sulforodamine labeled caspase inhibitor (SR-VAD-FMK), we discovered the pro-apoptotic action of the Cu(II) complex of alloferon and its analogues (injected in a dose of 10 nmol per insect) on hemocytes of *T. molitor*. We measured the fluorescence intensity of the labeled caspase inhibitor-caspase complex in hemocytes to quantify caspase activity, and we found that the degree of activation depended on the injected compounds (Table 7, Figure 6). The Cu(II) complex of alloferon 1 showed a 49% higher pro-apoptotic effect in hemocytes relative to alloferon, whereas two other tested compounds, (H6A) (Allo6A) and its Cu(II) complex, induced the activity of caspase in the same degree as native peptide. The most active was the Cu(II)−Allo12A analogue; it exhibited 123% higher caspase activity in hemocytes than native peptide, but the Allo12A analogue was practically inactive. At pH 7.4, a metal-to-ligand 1:1 molar ratio of Allo12A peptide with copper(II) ions forms the 4N $\{NH_2,N_{Im}\text{-}H^1,N_{Im}\text{-}H^6,N_{Im}H^9\}$ complex. This suggests that copper(II) ion coordinates the Allo12A peptide changing its conformation and its biological activity. As is seen in Figure S10 (CD spectra, Supporting Information), the coordination of the metal ions to the ligands studied changes the conformation of these peptides. The proportion of apoptotic hemocytes to all hemocytes tested increased after injection of the Cu(II)−Allo12A analogue (55%

dx.doi.org/10.1021/ic400160d | *Inorg. Chem.* 2013, 52, 5951−5961

Table 7. Pro-apoptotic Activity of Alloferon, Its Analogues, and Their Cu(II) Complexes in *T. molitor* Adults[a]

sample	no. of fluorescent cells counted	MFI ± SD	effect on the caspases activity relative to Allo1 (%)
RF	50	3.80 ± 0.86	0
MOPS	50	3.91 ± 0.86	0
MOPS + Cu	50	3.66 ± 1.42	0
Allo1	50	17.71 ± 3.15	100
Cu(II)−Allo1	50	26.31 ± 4.71	149
Cu(II)−Allo6A	50	16.85 ± 3.05	95
Allo6A	50	16.94 ± 1.88	95
Cu(II)−Allo12A	50	39.54 ± 6.35	223
Allo12A	50	3.88 ± 1.32	5

[a]The peptide, its analogue, or their Cu(II) complexes were injected in a dose of 10 nM (2 μL); the control insects were injected with the same volume of physiological solutions (RF), MOPS, or its Cu(II) complex. MFI, mean fluorescence intensity; SD, standard deviation.

of hemocytes displayed caspase activity) when compared to native peptide and its Cu(II) complex (50% of activated hemocytes), and it decreased after injection of Allo6A or its Cu(II) complex (30% of activated hemocytes) (Figure 7). The biological results show that Cu(II) *in vivo* did not cause any apparent apoptotic features in *T. molitor* cells but Cu(II) complexes of alloferon induce apoptosis. It is the first report that the cooper peptides exert pro-apoptotic activity on insect hemocytes.

The apparent binding constant of the first binding site is estimated to be in the low micromolar range (6×10^{-6} M); then, at a Cu(II) and peptide concentration of 20 nM (as used in the study for the *in vivo* measurements), it may be suggested that the peptide and Cu(II) is not making the complex; hence, one can question if the biological effects are really due to the complex (Cu−peptide) or to a synergy of two independent effects (Cu and peptide). However, as is seen in Table 7 and Figure 7, the different caspase activities (Table 7) and percentages of apoptosis (Figure 7) for the free Cu(II) ions,

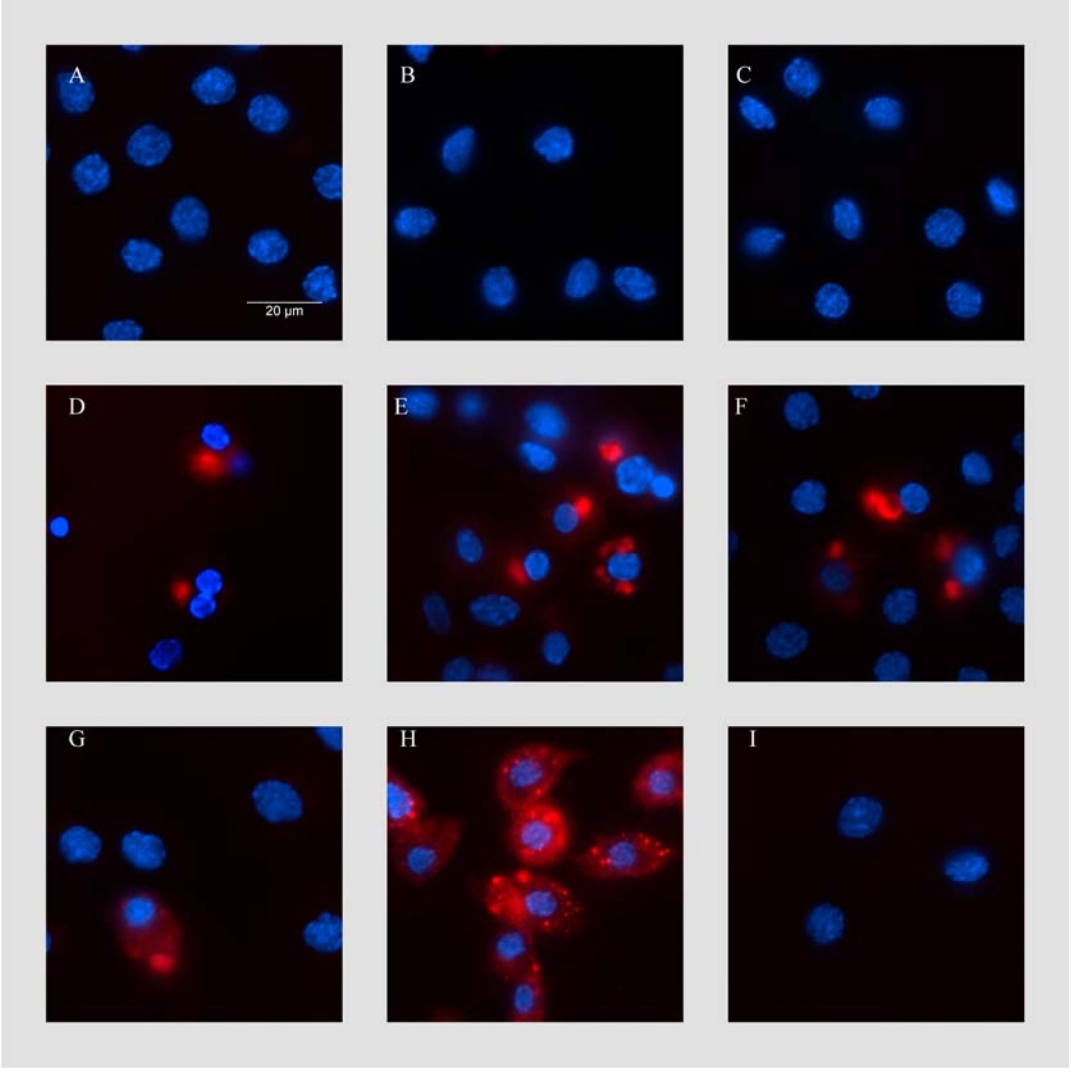

Figure 6. Representative fluorescence microscopic images showing *in vivo* induced apoptotic effects of alloferon, its analogues, and their Cu(II) complexes in *T. molitor* hemocytes. The peptide, its analogues, or their Cu(II) complexes were injected in a dose of 10 nM (2 μL), the control insects were injected with the same volume of physiological solutions (RF), MOPS, or its Cu(II) complex. All hemocytes were stained with SR-VAD-FMK reagent for caspase activity detection (red color) and DAPI for cell nuclei detection (blue color). A, RF; B, MOPS; C, MOPS + Cu(II); D, Allo 1; E, Cu(II) + Allo 1; F, Cu(II) + Allo6A; G, Allo6A; H, Cu(II)−Allo12A; I, Allo12A.

dx.doi.org/10.1021/ic400160d | *Inorg. Chem.* 2013, 52, 5951−5961

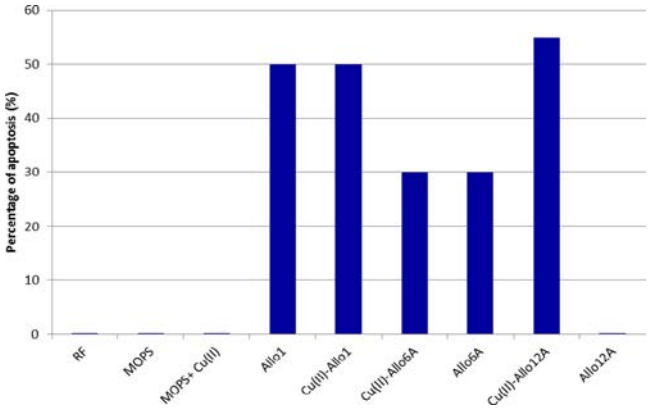

Figure 7. Percentage of apoptotic cells (number of fluorescent-apoptotic cells/number all cells × 100%) of alloferon, its analogues, and their Cu(II) complexes in *T. molitor* adults. The peptide, its analogue, or their Cu(II) complexes was injected in a dose of 10 nM (2 μL); the control insects were injected with the same volume of physiological solutions (RF), MOPS, or its Cu(II) complex.

free Allo12A peptide, and the Cu(II)−Allo12A complex may suggest the formation of the complex even in nanomolar concentration. It should be mentioned that the concentrations used in this study (free Cu(II) and Allo12A) were in the same range (20 nM).

CONCLUSION

Alloferons 1 with point mutations (H6A) and (H12A) studied here contain three histidine residues (H^1,H^9,H^{12} or H^1,H^6,H^9). The imidazole-N3 atom of the N-terminal His residue forms a stable 6-membered chelate with the terminal amine group. This interaction suppresses amide deprotonation (pK value above 8), but with increasing pH, sequential imidazole nitrogen atoms of histidine residues (H^9,H^{12} or H^6,H^9) are coordinated to copper(II) ions. For both peptides studied at physiological pH 7.4, the CuL complex dominates in the wide pH range 4.5−9.5 with the 4N {NH_2,N_{Im}-H^1,2N_{Im}} binding mode. In comparison to the Alloferon 1, the Allo6A and Allo12A have similar coordination abilities. The complex of Alloferon 1 with the 4N {NH_2,N_{Im}-H^1,2N_{Im}} binding mode is also present in the wide pH range 4.5−9. The value log K* for the 4N {NH_2,N_{Im}-H^1,2N_{Im}} complex of Alloferon 1 (−8.15) is similar to the value found for the complex of the Allo6A (−8.21), but this value is higher in comparison to that of the Allo12A (−8.91). It should be mentioned that the studies for the Alloferon 1 with point mutation (H9A) are now performed. For the metal-to-ligand 2:1 and 3:1 molar ratios at pH range 5.5−10.5, the di- and trinuclear complexes dominate, respectively, while at 3.5−5.5 mononuclear complexes are present. When the binding sites of the peptide are far enough from each other, the characteristic EPR spectrum may be observed. When deprotonation and metal ion coordination of amide functions takes place by increasing the pH, the EPR spectra of polynuclear complexes become very broad, indicating a short distance between the copper(II) ions and their involvement in metal−metal interactions.

The degree of caspase activation studied on hemocytes of *Tenebrio molitor* depended on the injected compounds. The Cu(II) complex of Alloferon 1 showed a 49% higher pro-apoptotic effect relative to Alloferon 1. The most active was the Cu(II)−Allo12A complex formed at pH 7.4 with 4N {NH_2,N_{Im}-H^1,N_{Im}-H^6,N_{Im}-H^9} binding sites. It exhibited 123% higher caspase activity in hemocytes than native peptide Allo 1. The difference between Allo1 and Cu(II)-Allo1 is not significant, but the difference between Allo12A and Cu(II)-Allo12A is significant.

ASSOCIATED CONTENT

Supporting Information

Concentration distributions of the complexes formed in the copper(II)−Allo12A system as a function of pH. UV−visible spectra of the Cu(II)−Allo6A 1:1 system at different pH values. Frozen solution EPR spectra of the complexes formed in the Cu(II)−Allo6A 1:1 and Cu(II)−Allo6A 3:1 systems. ESI mass spectra for the Cu(II)−Allo6A and Cu(II)-Allo12A systems at 1:1 molar ratio in water solution at pH about 7. Far-UV CD spectra of Allo6A (dashed lines) and Allo12A (solid lines) with and without copper(II) ions in MOPS buffer (pH 7.4). This material is available free of charge via the Internet at http://pubs.acs.org.

AUTHOR INFORMATION

Corresponding Author

*Phone: (048)(71) 375-72-31. Fax: (048) (71) 328-23-48. E-mail: teresa.kowalik-jankowska@chem.uni.wroc.pl.

Notes

The authors declare no competing financial interest.

ACKNOWLEDGMENTS

Financial support from the Polish Ministry of Science and Higher Education Grant NN 204085638 is gratefully acknowledged.

REFERENCES

(1) De Clerq, E. *Future Virol.* **2008**, *3*, 393−405.
(2) Lembo, D.; Cavalli, R. *Antiviral Chem. Chemother.* **2010**, *21*, 53−70.
(3) Kitazato, K.; Wang, Y.; Kobayashi, N. *Drug Discoveries Ther.* **2007**, *1*, 14−22.
(4) Field, H. J.; Biswas, S. *Drug Resist. Updates* **2011**, *14*, 45−51.
(5) Bhuwan, B. M.; Vinod, K. T. *Eur. J. Med. Chem.* **2011**, *46*, 4769−4807.
(6) Ratcliffe, N. A.; Mello, C. B.; Gracia, E. S.; Butt, T. M.; Azambuja, P. *Insect. Biochem. Mol. Biol.* **2011**, *41*, 747−769.
(7) Slocinska, M.; Marciniak, P.; Rosinski, G. *Protein Pept. Lett.* **2008**, *15*, 578−585.
(8) Chernysh, S.; Kim, S. I.; Bekker, G.; Filatove, V. A. A.; Anilin, V. B.; Platonom, V. G.; Bulle, P. *Proc. NATO Acad. Sci. USA* **2002**, *99*, 12628−12632.
(9) Ourth, D. D. *Biochem. Biophys. Res. Commun.* **2004**, *320*, 190−196.
(10) Kuczer, M.; Dziubasik, K.; Midak-Siwierska, A.; Zamorska, R.; Luczak, M.; Konopinska, D. *J. Pept. Sci.* **2010**, *16*, 186−192.
(11) Donald, D. O. *Peptides* **2010**, *31*, 1409−1411.
(12) Albiol Matanic, V. C.; Castilla, V. *Int. J. Antimicrob. Agents* **2004**, *23*, 382−389.
(13) Wang, G.; Watson, K. M.; Peterkofsky, A.; Buckheit, R. W., Jr. *Antimicrob. Agents Chemother.* **2010**, *54*, 1343−1346.
(14) Ryu, M. J.; Anikin, V.; Hong, S. H.; Jeon, H.; Yu, Y. G.; Yu, M. H. *Mol. Cell. Biochem.* **2008**, *313*, 91−102.
(15) Kuczer, M.; Midak-Siewierska, A.; Zahorska, R.; Luczak, M.; Konopinska, D. *J. Pept. Sci.* **2011**, *17*, 715−719.
(16) Kuczer, M.; Majewska, A.; Zahorska, R. *Chem. Biol. Drug Des.* **2013**, *81*, 302−309.
(17) Kozłowski, H.; Bal, W.; Dyba, M.; Kowalik-Jankowska, T. *Coord. Chem. Rev.* **1999**, *183*, 319−346.

(18) Sovago, I.; Varnagy, K.; Osz, K. *Comments Inorg. Chem.* **2002**, *23*, 149−178.
(19) Varnagy, K.; Szabo, J.; Sovago, I.; Malandrinos, G.; Hadjiliadis, N.; Sanna, D.; Micera, G. *J. Chem. Soc., Dalton Trans.* **2000**, 467−472.
(20) Kozlowski, H.; Kowalik-Jankowska, T.; Jezowska-Bojczuk, M. *Coord. Chem. Rev.* **2005**, *249*, 2323−2334.
(21) Sovago, I. Metal complexes of peptides and their derivatives. In Burger, K., Ed.; *Biocoordination Chemistry*; Allis Horwood: Chichester, 1990.
(22) Osz, K.; Nagy, Z.; Pappalardo, G.; Di Natale, G.; Sanna, D.; Micera, G.; Rizzarelli, E.; Sovago, I. *Chem.—Eur. J.* **2007**, *13*, 7129−7143.
(23) Kallay, C.; Varnagy, K.; Malandrinos, G.; Hadjiliadis, N.; Sanna, D.; Sovago, I. *Dalton Trans.* **2006**, 4545−4552.
(24) Damante, Ch. A.; Osz, K.; Nagy, Z.; Pappalardo, G.; Grasso, G.; Impellizzeri, G.; Rizzarelli, E.; Sovago, I. *Inorg. Chem.* **2008**, *47*, 9669−9683.
(25) Di Natale, G.; Osz, K.; Nagy, Z.; Sanna, D.; Micera, G.; Pappalardo, G.; Sovago, I.; Rizzarelli, E. *Inorg. Chem.* **2009**, *48*, 4239−4250.
(26) Kowalik-Jankowska, T.; Jezierska, J.; Kuczer, M. *Dalton Trans.* **2010**, *39*, 4117−4125.
(27) Kuczer, M.; Pietruszka, M.; Kowalik-Jankowska, T. *J. Inorg. Biochem.* **2012**, *111*, 40−49.
(28) Kochman, K.; Gajewska, A.; Kochman, H.; Kozłowski, H.; Masiukiewicz, E.; Rzeszotarska, B. *J. Inorg. Biochem.* **1997**, *65*, 277−279.
(29) Herman, A.; Kozłowski, H.; Czauderna, M.; Kochman, K.; Kulon, K.; Gajewska, A. *J. Physiol. Pharm.* **2012**, *63*, 69−75.
(30) Czarniewska, E.; Mrówczynska, L.; Kuczer, M.; Rosiński, G. *J. Exp. Biol.* **2012**, *215*, 4308−4313.
(31) Kuczer, M.; Czarniewska, E.; Rosiński, G. *Regul. Pept.* **2013**, *183*, 17−22.
(32) Marzano, C.; Pellei, M.; Tisato, F.; Santini, C. *Anti-Cancer Agents Med. Chem.* **2009**, *9*, 185−211.
(33) Habbeebu, S. S.; Liu, J.; Klaassen, C. D. *Toxicol. Appl. Pharmacol.* **1998**, *149* (2), 203−209.
(34) Raes, H.; Braekman, B. P.; Criel, G. R. J.; Rzeznik, U.; Vanfleteren, J. R. *J. Exp. Zool.* **2000**, *286*, 1−12.
(35) Lee, S. H.; Kim, D. K.; Seo, Y. R.; Woo, K. M.; Kim, C. S.; Cho, M. H. *Exp. Mol. Med.* **1998**, *30*, 171−176.
(36) Irving, H.; Miles, M. G.; Pettit, L. D. *Anal. Chim. Acta* **1967**, *38*, 475−488.
(37) Gans, P.; Sabatini, A.; Vacca, A. *J. Chem. Soc., Dalton Trans.* **1985**, 1195−1199.
(38) Gans, P.; Sabatini, A.; Vacca, A. *Talanta* **1996**, *43*, 1739−1753.
(39) Gran, G. *Acta Chem. Scand.* **1950**, *4*, 559−577.
(40) Rosinski, G.; Wrzeszcz, A.; Obuchowicz, L. *Insect Biochem* **1979**, *9*, 485−488.
(41) Ludwig, D.; Fiore, C. *Ann. Entomol. Soc. Am.* **1960**, *53*, 595−600.
(42) Ludwig, D.; Fiore, C.; Jones, R. *Ann. Entomol. Soc. Am.* **1962**, *55*, 439−442.
(43) Rosinski, G. *Zoololgical Series*; Adam Mickiewicz University Press: Poznan, 1995; Vol. *22*, p 148.
(44) Good, N. E.; Winget, G. D.; Winter, W.; Connolly, T. N.; Izawa, S.; Singh, R. M. M. *Biochemistry* **1966**, *5*, 467−477.
(45) Kuczer, M.; Czarniewska, E.; Rosiński, G.; Lisowski, M. *Peptides* **2013**, DOI: 10.1016/j.peptides.2013.04.002.
(46) Kowalik-Jankowska, T.; Jasionowski, M.; Lankiewicz, L. *J. Inorg. Biochem.* **1999**, *76*, 63−70.
(47) Jakab, N. I.; Gyurcsik, B.; Kortvelyesi, T.; Vosekalana, I.; Jensen, J.; Arsen, E. *J. Inorg. Biochem.* **2007**, *101*, 1376−1385.
(48) Kowalik-Jankowska, T.; Jankowska, E.; Szewczuk, Z.; Kasprzykowski, F. *J. Inorg. Biochem.* **2010**, *104*, 831−842.
(49) La Mendola, D.; Farkas, D.; Bellia, F.; Magri, A.; Travaglia, A.; Hansson, O.; Rizzarelli, E. *Inorg. Chem.* **2012**, *51*, 128−141.
(50) Arus, D.; Jancso, A.; Szunyogh, D.; Matyuska, F.; Nagy, V. N.; Hoffman, E.; Kortvelyesi, T.; Gajda, T. *J. Inorg. Biochem.* **2012**, *106*, 10−18.
(51) Sanna, D.; Micera, G.; Kally, Cs.; Rigo, V.; Sovago, I. *Dalton Trans.* **2004**, 2702−2707.
(52) Galey, J.-F.; Decock-Le Reverend, B.; Lebkiri, A.; Pettit, L. D.; Pyburn, S. I.; Kozlowski, H. *J. Chem. Soc., Dalton Trans.* **1991**, 2281−2287.
(53) Bal, W.; Dyba, M.; Kasprzykowski, F.; Kozłowski, H.; Latajka, R.; Lankiewicz, L.; Mackiewicz, Z.; Pettit, L. D. *Inorg. Chim. Acta* **1998**, *283*, 1−11.
(54) Kowalik-Jankowska, T.; Biega, L.; Kuczer, M.; Konopinska, D. *J. Inorg. Biochem.* **2009**, *103*, 135−142.
(55) Sovago, I.; Farkas, E.; Gergely, A. *J. Chem. Soc., Dalton Trans.* **1982**, 2159−2163.
(56) Sovago, I.; Petocz, G. *J. Chem. Soc., Dalton Trans.* **1987**, 1717−1720.
(57) Fawcett, T. G.; Bernarducci, E. E.; Krogh-Jespersen, K.; Schugar, H. J. *J. Am. Chem. Soc.* **1980**, *102*, 2598−2604.
(58) Alies, B.; Bijani, Ch.; Sayen, S.; Guillon, E.; Faller, P.; Hureau, Ch. *Inorg. Chem.* **2012**, *51*, 12988−13000.
(59) Phan, C. V.; Tosi, L.; Garnier, A. *Bioinorg. Chem.* **1978**, *8*, 21−31.
(60) Jansco, A.; Paksi, Z.; Jakab, N.; Gyurcsik, B.; Rockenbauer, A.; Gajda, T. *Dalton Trans.* **2005**, 3187−3194.
(61) Valensin, D.; Luczkowski, M.; Mancini, F. M.; Legowska, A.; Gaggelli, E.; Valensin, G.; Rolka, K.; Kozlowski, H. *Dalton Trans.* **2004**, 1284−1293.
(62) Kowalik-Jankowska, T.; Ruta-Dolejsz, M.; Wisniewska, K.; Lankiewicz, L. *J. Inorg. Biochem.* **2002**, *92*, 1−10.
(63) Kowalik-Jankowska, T.; Ruta, M.; Wisniewska, K.; Lankiewicz, L. *J. Inorg. Biochem.* **2003**, *95*, 270−282.
(64) Kowalik-Jankowska, T.; Ruta-Dolejsz, M.; Wisniewska, K.; Lankiewicz, L. *J. Inorg. Biochem.* **2001**, *86*, 535−545.
(65) Gajda, T.; Henry, B.; Aubry, A.; Delpuech, J.-J. *Inorg. Chem.* **1996**, *35*, 586−593.
(66) Moini, M. *Rapid Commun. Mass Spectrom.* **2010**, *24*, 2730−2734.
(67) Keith-Roach, M. *Anal. Chim. Acta* **2010**, *678*, 140−148.
(68) Rajkovic, S.; Kallay, C.; Serenyi, R.; Malandrinos, G.; Hadjiliadis, N.; Sanna, D.; Sovago, I. *Dalton Trans.* **2008**, 5059−5071.
(69) Sovago, I.; Osz, K. *Dalton Trans.* **2006**, 3841−3854.
(70) Timari, S.; Kallay, C.; Osz, K.; Sovago, I.; Varnagy, K. *Dalton Trans.* **2009**, 1962−1971.
(71) Stern, C. A.; Gennaro, A. M.; Levstein, P. R.; Calvo, R. J. *Phys. Condens. Matter* **1989**, *1*, 637−642.
(72) Anderson, P. W. *Phys. Soc. Jpn.* **1954**, *9*, 316−339.
(73) Glaser, T.; Heidemeier, M.; Hahn, F. E.; Lugger, T. *Z. Naturforsch.* **2003**, *58b*, 505−510.